Inorganic Chemistry

Article

pubs.acs.org/IC

Five-Stage Near-Infrared Electrochromism in Electropolymerized Films Composed of Alternating Cyclometalated Bisruthenium and Bis-triarylamine Segments

Chang-Jiang Yao,[†,‡] Yu-Wu Zhong,*[,†,§] and Jiannian Yao[†]

[†]Beijing National Laboratory for Molecular Sciences, CAS Key Laboratory of Photochemistry, Institute of Chemistry, Chinese Academy of Sciences, Beijing 100190, China

[‡]University of Chinese Academy of Sciences, Beijing 100049, China

[§]State Key Laboratory of Coordination Chemistry, Nanjing University, Nanjing 210093, China

Supporting Information

ABSTRACT: Oxidative electropolymerization of cyclometalated bisruthenium complexes $[(Nptpy)_2Ru_2(tppyr)](PF_6)_2$ and $[(Nptpy)_2Ru_2(tpb)](PF_6)_2$ produced adherent metallopolymeric films on electrode surfaces, where Nptpy is 4′-(*p*-*N*,*N*-diphenylamino)phenyl-2,2′:6′,2″-terpyridine, tppyr is the 2,7-bisdeprotonated form of 1,3,6,8-tetra(pyrid-2-yl)-pyrene, and tpb is the 3,6-bisdeprotonated form of 1,2,4,5-tetra(pyrid-2-yl)benzene. The resulting polymers are composed of two types of alternating constituent units: tppyr- or tpb-bridged cyclometalated bisruthenium units and biphenyl-bridged bis-triarylamine segments. These films exhibited four well-defined anodic redox couples as a result of the stepwise oxidations of these two units. By manipulating the intervalence charge-transfer transitions of mixed-valent bisruthenium and bis-triarylamine units, five-stage near-infrared electrochromism with stepwise color changes accompanied by good contrast ratio and coloration efficiency has been realized in these films. The film characterization by scanning electronic microscopy and X-ray photoelectron spectroscopy techniques are presented as well.

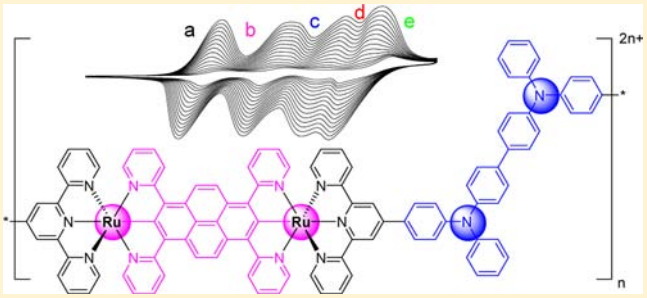

INTRODUCTION

Materials with well-defined multiple redox states are of interest for electrochromism,[1] information storage, and molecular electronics.[2] For practical applications, polymeric films with long-term stability, good contrast ratio, and low switching potential are desired. Routine film formation methods include spin-coating, drop-casting, layer-by-layer assembly,[3] and electropolymerization accompanied by in situ film coatings.[4] Among these methods, electropolymerization offers several advantages. Polymer formation and film deposition are achieved simultaneously, which shortens the experimental time and avoids the solubility problems often met in other methods. In addition, the surface coverage of electropolymerized films can be easily controlled.

Metal oxides,[5] organic conducting polymers,[4a,b,6] and coordination metallopolymers[4c,7] are frequently used for electrochromic studies. These materials often exhibit electrochromism in the visible region. Polymeric films that display distinctly different absorptions in the near-infrared (NIR, 800–2000 nm) region at different redox states are much less well-known,[8] although they are of great importance in many military and civilian uses.[9] In this regard, Liou and co-workers have reported a series of triarylamine-based polyamides that display excellent NIR electrochromic behaviors.[10] The NIR absorptions of these materials arise from the intervalence charge transfer (IVCT) transitions of mixed-valent bis-triarylamine units or charge-resonance bands in the case of Robin–Day class III systems.[11] Using reductive electropolymerization of vinyl-substituted polypyridine complexes,[12] we have recently prepared some metallopolymeric films consisting of biscyclometalated ruthenium segments.[13] These films exhibited promising NIR electrochromic behaviors with good contrast ratio. The electrochromic switching can be operated at rather low voltages thanks to the strong metal–ligand orbital mixing and readily oxidizable nature of cyclometalated ruthenium complexes.[14] The wavelength of the NIR absorptions can be varied by changing the bridging ligand. The NIR absorptions arise from the IVCT transitions between two mixed-valent ruthenium sites.

All of the above-mentioned materials contain one or two redox processes. The development of materials displaying more than three redox processes and thus multistage electrochromic behaviors remains a challenging task.[15] These materials are very useful for some practical applications such as color displays, optical communication, and e-papers.[16] Linear assembly of multiple redox sites into one molecule will in principle give rise to materials with multiple redox process. However, this method

Received: May 22, 2013
Published: August 9, 2013

dx.doi.org/10.1021/ic401288g | *Inorg. Chem.* 2013, 52, 10000–10008

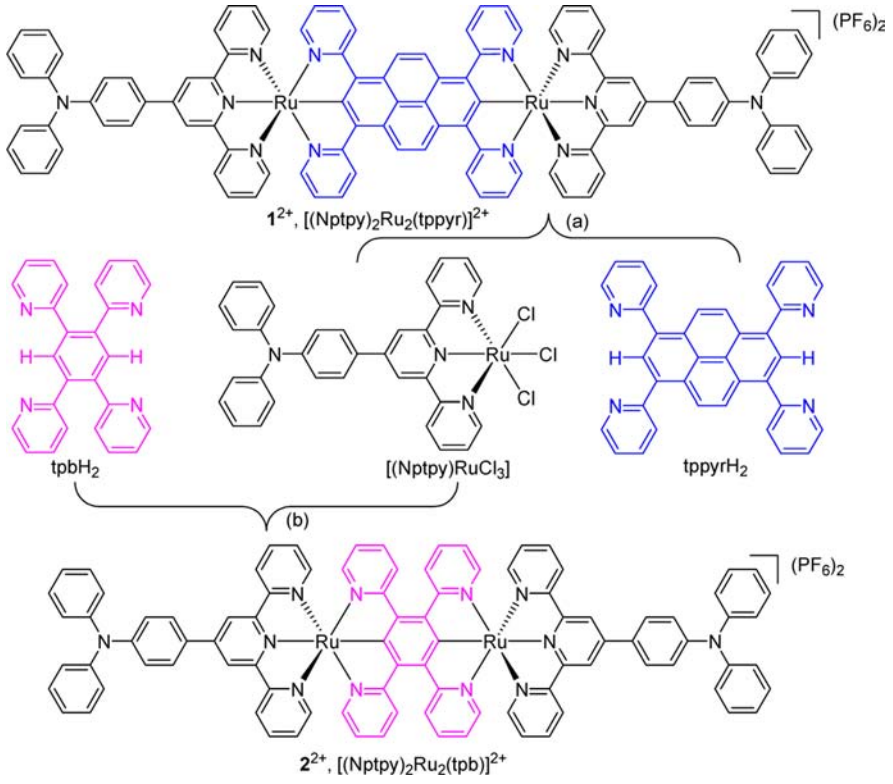

Figure 1. Synthesis of $\mathbf{1}^{2+}$ and $\mathbf{2}^{2+}$. Conditions: (a) (1) AgOTf; (2) KPF_6, 44%. (b) (1) AgOTf; (2) KPF_6, 43%.

often fails because of the extreme difficulty in obtaining materials with strong electronic coupling between two terminal redox sites.[17] In another aspect, materials with multiple redox processes does not necessarily give rise to intense absorptions in the NIR region. In this contribution, we present a conceptually new strategy to access such materials and films. We envisaged that when a bisruthenium complex with two terminal diphenyl amino groups was subjected to head-to-tail electropolymerization, the polymeric film could be deposited on electrode surfaces accompanied by the formation of biphenyl-bridged bis-amine units. As a result, the new polymeric materials are composed of alternating bisruthenium and bis-triarylamine segments, and the generation of multistage NIR electrochromism is possible by manipulating the IVCT bands of two constituent components. However, the realization of such strategy must meet several important prerequisites. The redox potentials associated with the bisruthenium components must be low and well-separated from those of the bis-amine units. The IVCT bands of the bisruthenium and bis-triarylamine segments must have different wavelength to distinguish individual step spectral changes. Besides, care must be taken during the electropolymerization experiments and special techniques are to be invoked if necessary, because the formation of polymers from triphenylamine is well-known to be difficult through conventional electrochemical methods.[18]

RESULTS AND DISCUSSION

To test the feasibility of the above strategy, we have designed two compounds $[(Nptpy)_2Ru_2(tppyr)](PF_6)_2$ (Figure 1, $\mathbf{1}^{2+}$) and $[(Nptpy)_2Ru_2(tpb)](PF_6)_2$ ($\mathbf{2}^{2+}$), which were synthesized from the complexation of $[Ru(Nptpy)Cl_3]$ (Nptpy = 4′-(*p*-*N*,*N*-diphenylamino)phenyl-2,2′:6′,2″-terpyridine) with 1,3,6,8-tetra(pyrid-2-yl)pyrene ($tppyrH_2$)[19] and 1,2,4,5-tetra(pyrid-2-yl)benzene ($tpbH_2$)[20] in acceptable yield. In these complexes, tppyr is the 2,7-bisdeprotonated form of $tppyrH_2$, and tpb is the 3,6-bisdeprotonated form of $tpbH_2$. They both act as a biscyclometalating bridging ligand to connect two ruthenium sites. The previous reported model compounds $[(tpy)_2Ru_2(tppyr)](PF_6)_2$[19] (tpy = 2,2′:6′,2″-terpyridine) and $[(tpy)_2Ru_2(tpb)](PF_6)_2$[20] without the terminal triphenylamine groups exhibit the IVCT transitions centered around 2100 and 1160 nm, respectively, in their singly oxidized forms. Meanwhile, the IVCT transition of the mixed-valent bis-triarylamine system with the biphenyl backbone is around 1550 nm,[21] which is well separated from those arising from the bisruthenium units. We thus expected that the polymeric films formed by head-to-tail electropolymerization of $\mathbf{1}^{2+}$ and $\mathbf{2}^{2+}$ would exhibit distinctly multistep spectral changes in the NIR region, as a result of switching the IVCT transitions of the bisruthenium and bis-triarylamine units.

Complex $\mathbf{1}^{2+}$ in CH_2Cl_2 displays two consecutive anodic redox waves at +0.48 and +0.70 V vs Ag/AgCl, as shown by the steady-state cyclic voltammogram (CV) in Figure 2a. Similar electrochemical behaviors have been observed for $[(tpy)_2Ru_2(tppyr)](PF_6)_2$.[19] These waves are ascribed to the stepwise $Ru^{II/III}$ processes mixing with some amount of bridging-ligand oxidation. When the potential was scanned repeatedly between 0 and +1.3 V vs Ag/AgCl at a Pt disk electrode, the current in the CV increased gradually and continuously and two new redox peaks appeared at +0.88 and +1.00 V in addition to the slightly negative-shifted $Ru^{II/III}$ processes. This indicated that the oxidative electropolymerization of $\mathbf{1}^{2+}$ in CH_2Cl_2 proceeded smoothly on the Pt electrode surface. The new peaks at +0.88 and +1.00 V are associated with the stepwise oxidations of the bis-triarylamine segments in the polymers. However, the electropolymerization did not proceed in CH_3CN because of limited solubility of $\mathbf{1}^{2+}$ in CH_3CN in the presence of the electrolyte used ($^nBu_4NClO_4$).

dx.doi.org/10.1021/ic401288g | Inorg. Chem. 2013, 52, 10000−10008

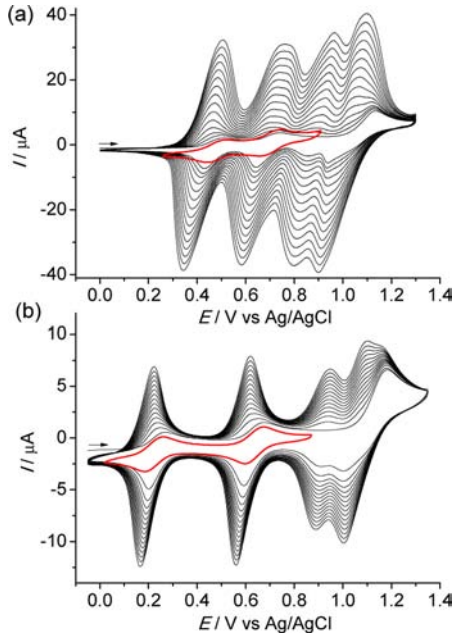

Figure 2. Oxidative electropolymerization of (a) $\mathbf{1}^{2+}$ (0.5 mM in CH_2Cl_2) and (b) $\mathbf{2}^{2+}$ (0.2 mM in CH_2Cl_2) on a Pt disk electrode by 15 repeated potential scan cycles at 100 mV/s. The plots in red color are the steady state electrochemical response of $\mathbf{1}^{2+}$ and $\mathbf{2}^{2+}$ in the potential window of 0.30−0.90 V and 0−0.90 V, respectively.

Complex $\mathbf{2}^{2+}$ shows two $Ru^{II/III}$ processes at +0.22 and +0.63 V vs Ag/AgCl (Figure 2b), similar to the previously reported model complex $[(tpy)_2Ru_2(tpb)](PF_6)_2$.[20] As for the electropolymerization, complex $\mathbf{2}^{2+}$ proceeded smoothly as well when the potential was scanned beyond the oxidation of the triphenylamine group (Figure 2b). The newly appeared N/N$^+$ waves at +0.90 and +1.04 V are in the same region with those of the poly-$\mathbf{1}^{2+}$ film.

The electropolymerization of $\mathbf{1}^{2+}$ and $\mathbf{2}^{2+}$ took place equally well on indium−tin-oxide (ITO) glass electrodes with a typical geometrical dimension of 20 mm × 8 mm (Figure 3). Figure 3b shows the CVs of a produced polymeric film at different scan rates in a clean electrolyte solution (surface coverage $\Gamma = 1.3 \times 10^{-9}$ mol/cm^2). Four well-defined redox couples are observed. The potential separations between the anodic and cathodic waves of each redox couple are less than 59 mV at slow scan rates. However, these separations become larger at faster scan rates (e.g., 30 mV at 10 mV/s and 190 mV at 100 mV/s, respectively, for the first redox wave). Both anodic and cathodic currents are linearly dependent on the scan rate (Figure 3c), which is characteristic of redox processes confined on electrode surfaces. The surface coverage of the polymeric films could be easily varied by changing the electropolymerization duration (Figure 3d). The peak-to-peak potential separations between the anodic and cathodic waves of each redox couple increased as the polymer film thickened, possibly as a result of the increased resistance of the film.

When 1 equiv of oxidant (cerium ammonium nitrate, CAN) was added to a solution of $\mathbf{1}^{2+}$, a broad IVCT absorption band centered at 2100 nm appeared (Supporting Information, Figure S1). This band decreased and disappeared when up to 2 equiv of CAN was added. The NIR absorption spectral changes of $\mathbf{2}^{2+}$ during the oxidative titration with CAN are shown in Supporting Information, Figure S2, which evidence the appearance and disappearance of the IVCT band at 1160 nm after single- and double-oxidation, respectively. The attachment of the triphenylamine groups on $[(tpy)_2Ru_2(tppyr)]^{2+}$ and $[(tpy)_2Ru_2(tpb)]^{2+}$ did not shift the IVCT absorption maxima of their mixed-valent state.

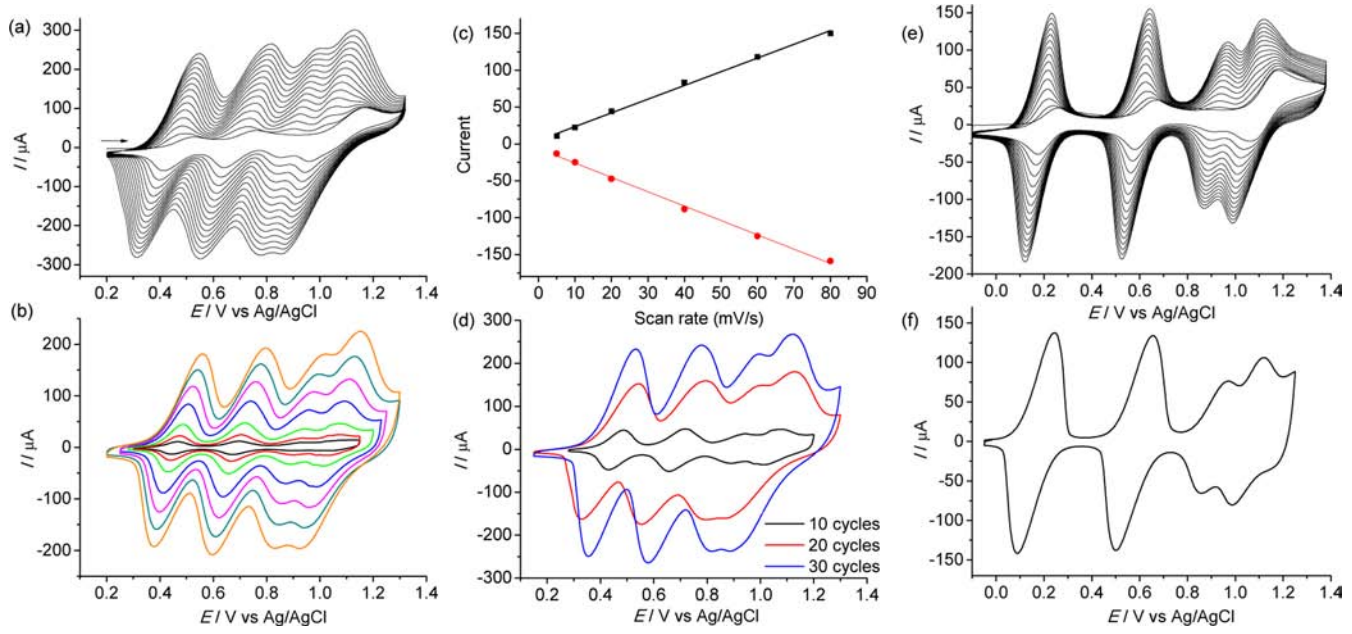

Figure 3. (a) Oxidative electropolymerization of $\mathbf{1}^{2+}$ (0.5 mM in CH_2Cl_2) on an ITO glass electrode by 15 repeated potential scan cycles between +0.2 and +1.3 V at 100 mV/s. (b) CVs of poly-$\mathbf{1}^{2+}$/ITO films obtained in (a) at different scan rates (5, 10, 20, 40, 60, 80, and 100 mV/s, respectively). (c) Linear dependence of peak currents of the first redox wave in (b) as a function of scan rate. The R^2 values are 0.99584 and 0.99651 for the anodic and cathodic currents, respectively. (d) CVs of poly-$\mathbf{1}^{2+}$/ITO films obtained after 10, 20, and 30 electropolymerization cycles. The scan rate was 20 mV/s. (e) Oxidative electropolymerization of $\mathbf{2}^{2+}$ (0.2 mM in CH_2Cl_2) on an ITO glass electrode by 15 repeated potential scan cycles between −0.1 and +1.4 V at 100 mV/s. (f) CV of poly-$\mathbf{2}^{2+}$/ITO film obtained in (e) at the scan rate of 100 mV/s.

dx.doi.org/10.1021/ic401288g | Inorg. Chem. 2013, 52, 10000−10008

Figure 4 shows the representative absorption spectral changes of poly-$\mathbf{1}^{2+}$/ITO film upon stepwise applying potentials from +0.20 to +1.26 V vs Ag/AgCl. When the potential was gradually increased to +0.56 V to induce the first one-electron oxidation of the bisruthenium units, broad IVCT transitions between 1500 and 3000 nm increased (Figure 4a). This band decreased until it disappeared upon further increasing the potential to +0.76 V to induce the second one-electron oxidation of the bisruthenium units (Figure 4b). Upon further increasing the potential to +0.96 V, the bis-triarylamine units in the polymers began to be oxidized, and an IVCT band between the mixed-valent amines appeared at 1500 nm (Figure 4c). This band decreased again when both amine units were oxidized upon increasing the potential to +1.26 V (Figure 4d). These four-step (five-stage) spectral changes are fully reversible when the applied potential was reversed. In the first and second step, the color of the film changed from dark blue to brown and then to orange. No significant color changes were evident during the last two-step changes.

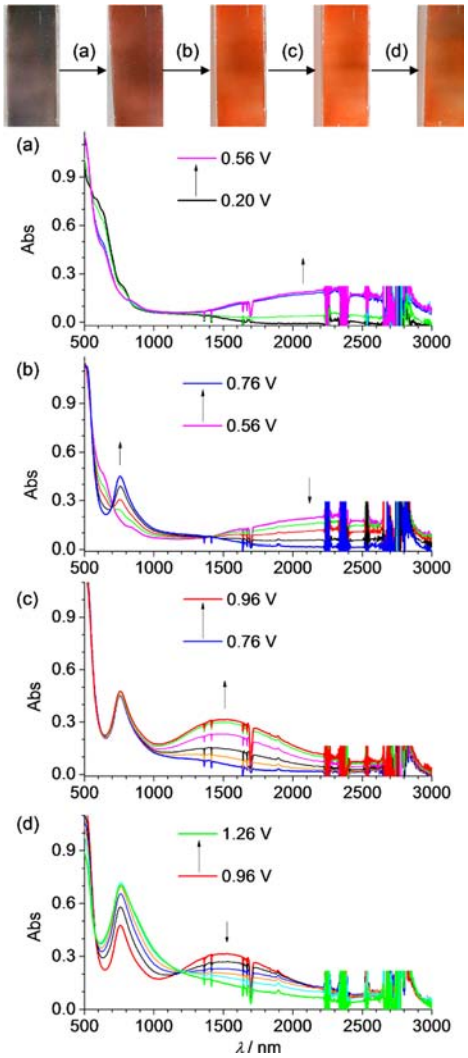

Figure 4. Absorption spectral changes of a poly-$\mathbf{1}^{2+}$ film on ITO glass ($\Gamma = 4.2 \times 10^{-9}$ mol/cm^2) upon stepwise applying potentials from (a) +0.20 to +0.56 V, (b) +0.56 to +0.76 V, (c) +0.76 to +0.96 V, and (d) +0.96 to +1.26 V vs Ag/AgCl. The plot on the top shows the film with different colors in different states.

The multistep electrochromic behavior of above poly-$\mathbf{1}^{2+}$/ITO film was further examined by double-potential step chronoamperometry. Figure 5a and b shows the representative percent transmittance (T%) changes of a film ($\Gamma = 4.2 \times 10^{-9}$ mol/cm^2) at 2150 nm as a function of time when the potential was switched stepwise between +0.20 to +0.56 V and +0.56 to +0.76 V vs Ag/AgCl, respectively. This attests to the good film stability during these processes. The contrast ratios (ΔT%) for the first and second step electrochromism are rather small at a small surface coverage, but increase to an optimum value of more than 50% for both steps (Figure 6a and b). The coloration efficiency at 2150 nm for these two processes is about 550 cm^2/C at the optimum contrast ratio.[22] This performance is better than the previously polymeric films prepared via reductive electropolymerization of a vinyl-substituted bisruthenium complex with the same bridging ligand,[13b] where the best ΔT% value is around 35% and the coloration efficiency is around 220 cm^2/C. The response time for the contrast ratio to reach over 90% of its maximum is around 15−20 s (Figure 5e and f).

Figure 5c and d shows the T% changes of the same film at 1500 nm vs time when the potential was switched stepwise between +0.76 to +0.96 V and +0.96 to +1.26 V vs Ag/AgCl, respectively, to induce the stepwise oxidations of the bis-triarylamine units. The contrast ratio varies as the surface coverage changes. The best contrast ratio achieved is 27% and 23% for the third and fourth step electrochromism (Figure 6c and d). The response time is a few tens of seconds (Figure 5g and h). The coloration efficiency is about 100 cm^2/C. It should be noted that the contrast ratio for these two processes decreases gradually after some cycling (see also Supporting Information, Figure S3, for a film with a small surface coverage). When the polymeric film was applied at a constant potential of +1.3 V for 10 min, the $Ru^{II/III}$ peaks were retained, while the $N^{0/+}$ peaks significantly decreased. This suggests that the rapid loss of the activity associated with the $N^{0/+}$ process is possibly caused by oxidative degradation of the polymer at high positive potentials, rather than detachment of the film.

Figures 7 and 8 show the absorption spectral changes and transmittance switching of typical poly-$\mathbf{2}^{2+}$/ITO film upon stepwise application of potentials from +0.01 to +1.15 V vs Ag/AgCl. Again, this film displays reversible five-stage NIR electrochromism. However, because of the use of different bridging ligand (tpb vs tppyr) for the bisruthenium units, the first two step processes involve the spectral changes in a lower-energy region with respect to the poly-$\mathbf{1}^{2+}$ film (λ_{max}: 1185 vs 2150 nm). However, their third and fourth step switching processes, which are associated with the bis-triarylamine unit, essentially display the same spectral changes. The colors of the poly-$\mathbf{2}^{2+}$/ITO film in each stage are significantly different from those of the poly-$\mathbf{1}^{2+}$/ITO film. In the first and second stage, the poly-$\mathbf{2}^{2+}$/ITO film is blue and brown, respectively. In the last three stages, the film turns olive and then green.

The poly-$\mathbf{2}^{2+}$/ITO film with Γ of 5.5×10^{-9} mol/cm^2 exhibits steady-state ΔT% of 28%, 22%, and 35%, respectively, for their first to third step switching processes at the absorption maximum wavelength (Figure 8). The electrochemical stability for the fourth step switching process is somewhat low, as has been found in the above poly-$\mathbf{1}^{2+}$/ITO film. A film with a low Γ shows inferior performance (Supporting Information, Figure S4).

The film surface morphology was examined by scanning electron microscopy (SEM). Figure 9 shows a typical SEM

dx.doi.org/10.1021/ic401288g | Inorg. Chem. 2013, 52, 10000−10008

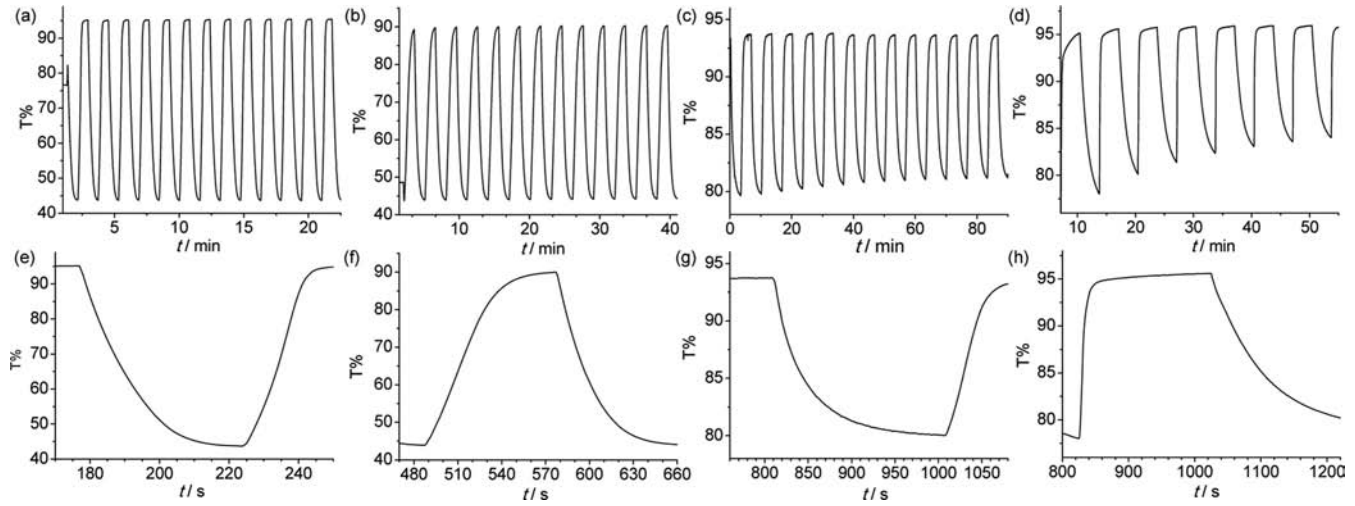

Figure 5. Transmittance switching of a poly-$\mathbf{1}^{2+}$/ITO film ($\Gamma = 4.2 \times 10^{-9}$ mol/cm^2) monitored at λ = (a,b,e,f) 2150 nm and (c,d,g,h) 1500 nm as a function of time (t) between (a,e) +0.20 and +0.56 V, (b,f) +0.56 and +0.76 V, (c,g) +0.76 and +0.96 V, and (d,h) +0.96 and +1.26 V vs Ag/AgCl in 0.1 M Bu_4NClO_4/CH_2Cl_2.

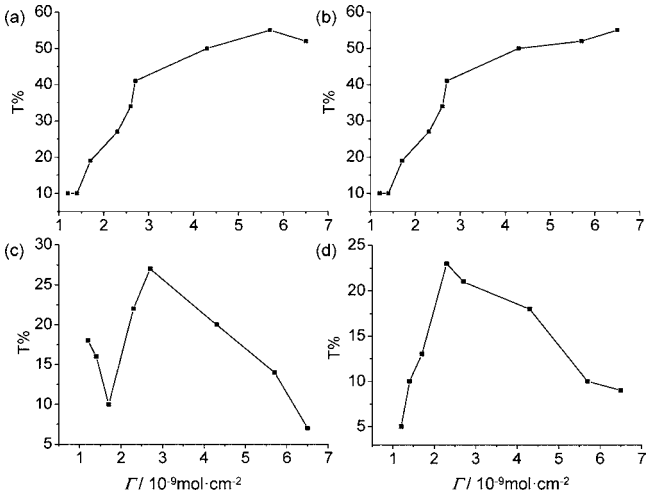

Figure 6. Plots of the contrast ratio (T%) vs surface coverage (Γ) for the (a) first, (b) second, (c) third, and (d) fourth step electrochromism of poly-$\mathbf{1}^{2+}$/ITO film.

picture of the poly-$\mathbf{2}^{2+}$/ITO film with Γ of 2.8×10^{-9} mol/cm^2. The polymeric layer adheres tightly to the ITO substrate. The surface evidence the presence of some irregular (mostly globular) textures in the order of tens to a few hundred nanometers. Apart from these domains, the film surface is essentially flat.

Figure 10 shows the X-ray photoelectron spectroscopy (XPS) survey spectra of poly-$\mathbf{1}^{2+}$/ITO and poly-$\mathbf{2}^{2+}$/ITO film. The Ru $3p_3$ and 3d signals around 462 and 281 eV are easily discerned. The poly-$\mathbf{1}^{2+}$ film has slightly lower Ru atom composition with respect to the poly-$\mathbf{2}^{2+}$ film (0.86% vs 1.03%). This trend is in accordance with the atom composition of their monomers.

The polymers of $\mathbf{1}^{2+}$ and $\mathbf{2}^{2+}$ obtained by electropolymerization are virtually insoluble in most organic solvents, such as acetonitrile, chloroform, dichloromethane, dimethyl sulfoxide, and *N*,*N*-dimethylformamide. Thus, the characterization of these materials by conventional NMR and mass spectroscopy is difficult. With the help of a small amount of trifluoroacetic acid, the poly-$\mathbf{1}^{2+}$ scratched off the ITO film is slightly soluble in acetonitrile (most of the sample is insoluble). The matrix-assisted laser desorption ionization time-of-flight (MALDI-TOF) mass spectrum of the dissolved material shows a signal at 3324 D, which is in accordance with a dimeric structure of $\mathbf{1}^{2+}$ after loss of counteranions and a few protons (Supporting Information, Figure S5).

Taking complex $\mathbf{2}^{2+}$ as an example, a possible electropolymerization mechanism is given in Figure 11. Upon electrochemical oxidation, the triphenylamine unit was transformed into a radical cation intermediate. After carbon−carbon bond formation on the para-position of terminal benzene rings, followed by a reductive de-doping process, the $\mathbf{2}^{2+}$-dimer was produced. The radical cation dimerization of triphenylamine to produce the tetraphenylbenzidine upon oxidation is well-known.[18] Upon further oxidation, the chain propagation very likely takes from the two terminal triphenylamine groups of the $\mathbf{2}^{2+}$-dimer to give poly-$\mathbf{2}^{2+}$. The middle tetraphenylbenzidine unit can be oxidized, even at less positive potential relative to triphenylamine, but it is very difficult for further electrochemical coupling because the charge is delocalized. This is also the reason why triphenylamine usually undergoes dimerization upon oxidation, but not polymerization.[18] However, if a molecule contains two triphenylamines on distal positions and there is little electronic coupling between them (just like complexes $\mathbf{1}^{2+}$ and $\mathbf{2}^{2+}$), the formation of polymeric films through the head-to-tail electropolymerization is possible.[23] Our work further demonstrates the generality of such transformation. It is possible that the film contains some short oligomers, if their solubility is very low and they quickly deposited on the electrode surface once formed. The structure of poly-$\mathbf{2}^{2+}$ is also supported by the electrochemical data, which shows two (and only two) well-defined N/N^+ waves. If the middle tetraphenylbenzidine of the $\mathbf{2}^{2+}$-dimer undergoes chain propagation, the N/N^+ potentials will be changed by the added triarylamine unit, and the N/N^+ waves will be more complex.

■ CONCLUSION

In conclusion, new polymeric films integrating both two-step redox-active inorganic and organic segments into one system have been prepared through oxidative electropolymerization of triphenylamine-substituted biscyclometalated ruthenium com-

dx.doi.org/10.1021/ic401288g | *Inorg. Chem.* 2013, 52, 10000−10008

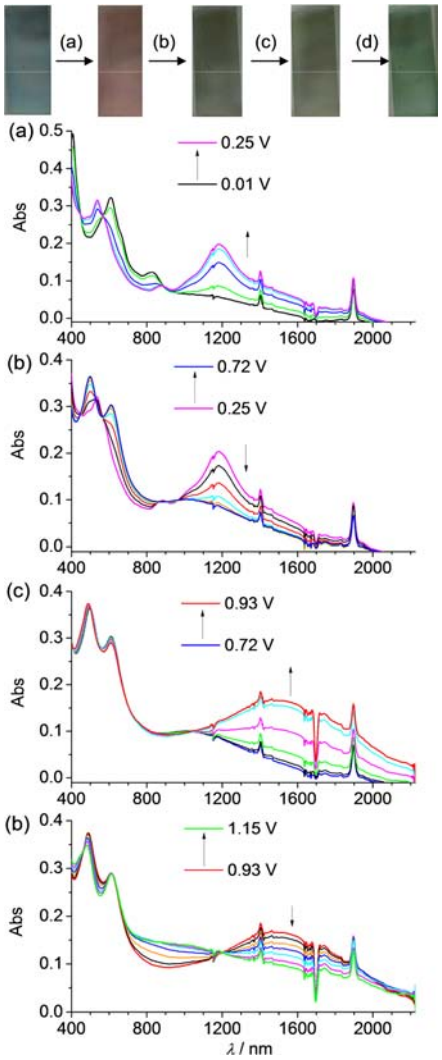

Figure 7. Absorption spectral changes of a poly-$\mathbf{2}^{2+}$/ITO film ($\Gamma = 1.0 \times 10^{-9}$ mol/cm^2) upon stepwise applying potentials from (a) +0.01 to +0.25 V, (b) +0.25 to +0.72 V, (c) +0.72 to +0.93 V, and (d) +0.93 to +1.15 V vs Ag/AgCl. The plot on the top shows the film with different colors in different states.

plexes. The resulting adherent metallopolymeric films display four-step well-defined anodic redox events arising from the bisruthenium and bis-triarylamine segments in the polymers. These films exhibit five-stage NIR electrochromism with good contrast ratio and coloration efficiency as a result of switching the IVCT bands of inorganic and organic mixed-valence units, respectively. The absorption wavelength of the electrochromism and the colors of the polymeric film at individual stages can be tuned by the use of a different bridging ligand of the bisruthenium unit. The electrochromic performance of these films will be susceptible to improvement.[24] Considering that a vast number of mixed-valence dimetallic complexes have been reported up to date,[25] our findings open a new avenue for preparing polymeric films with multistep redox processes and multistage NIR electrochromism.

EXPERIMENTAL SECTION

Spectroscopic Measurements. UV/vis/NIR spectra were recorded using a PerkinElmer Lambda 750 UV/vis/NIR spectrophotometer at room temperature in denoted solvents, with a conventional 1.0 cm quartz cell. Oxidative spectroelectrochemistry was performed in a thin layer cell (optical length = 0.2 cm) in which an ITO glass electrode was set in an indicated solvent containing 0.1 M Bu_4NClO_4 and the compound to be measured (the concentration is around 1×10^{-4} M). A platinum wire and Ag/AgCl in saturated aqueous solution was used as a counter electrode and a reference electrode. The cell was placed in a PE Lambda 750 UV/vis/NIR spectrophotometer to monitor spectral changes during electrolysis.

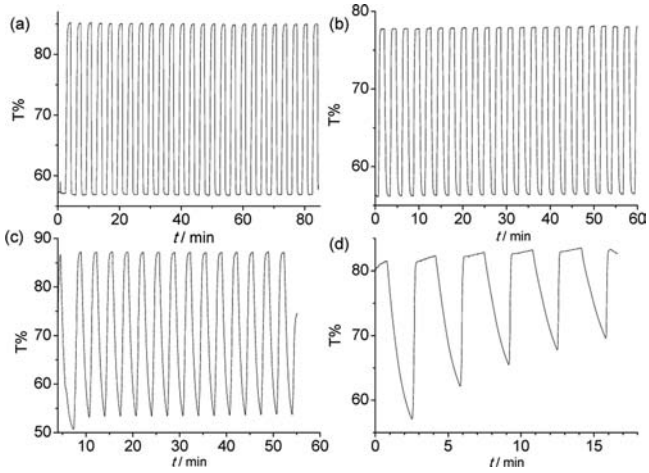

Figure 8. Transmittance switching of a poly-$\mathbf{2}^{2+}$/ITO film ($\Gamma = 5.5 \times 10^{-9}$ mol/cm^2) monitored at λ = (a,b) 1185 nm and (c,d) 1600 nm as a function of time (t) between (a) +0.01 and +0.43 V, (b) +0.43 and +0.70 V, (c) +0.70 and +0.93 V, and (d) +0.93 and +1.20 V vs Ag/AgCl in 0.1 M Bu_4NClO_4/CH_2Cl_2.

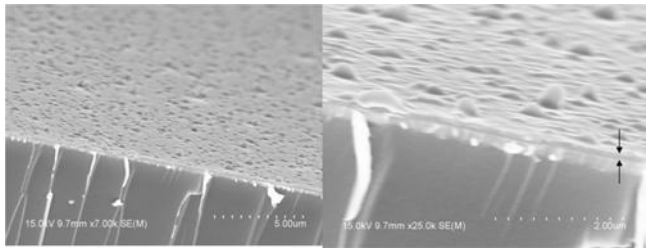

Figure 9. Representative SEM images of poly-$\mathbf{2}^{2+}$/ITO film ($\Gamma = 2.8 \times 10^{-9}$ mol/cm^2). The polymeric layer (around 100 nm) is indicated by arrows.

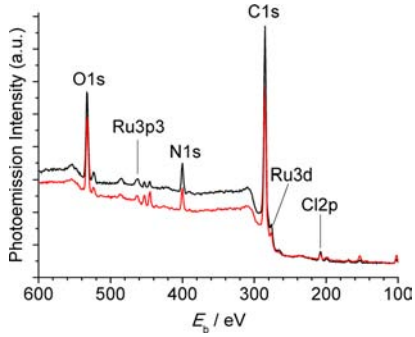

Figure 10. XPS survey spectra of poly-$\mathbf{1}^{2+}$/ITO (black curve) and poly-$\mathbf{2}^{2+}$/ITO (red curve) film.

Electropolymerization and Spectroelectrochemistry Measurement. The electropolymerization experiments were carried out using a CHI 620D potentiostat in 0.1 M of Bu_4NClO_4/CH_2Cl_2 with a Ag/AgCl reference electrode. The working electrode was a Pt disk electrode or an ITO glass electrode. A platinum coil is used as the counter electrode. The experiments were performed in a three-compartment electrochemical cell. The ITO glass was positioned

dx.doi.org/10.1021/ic401288g | Inorg. Chem. 2013, 52, 10000−10008

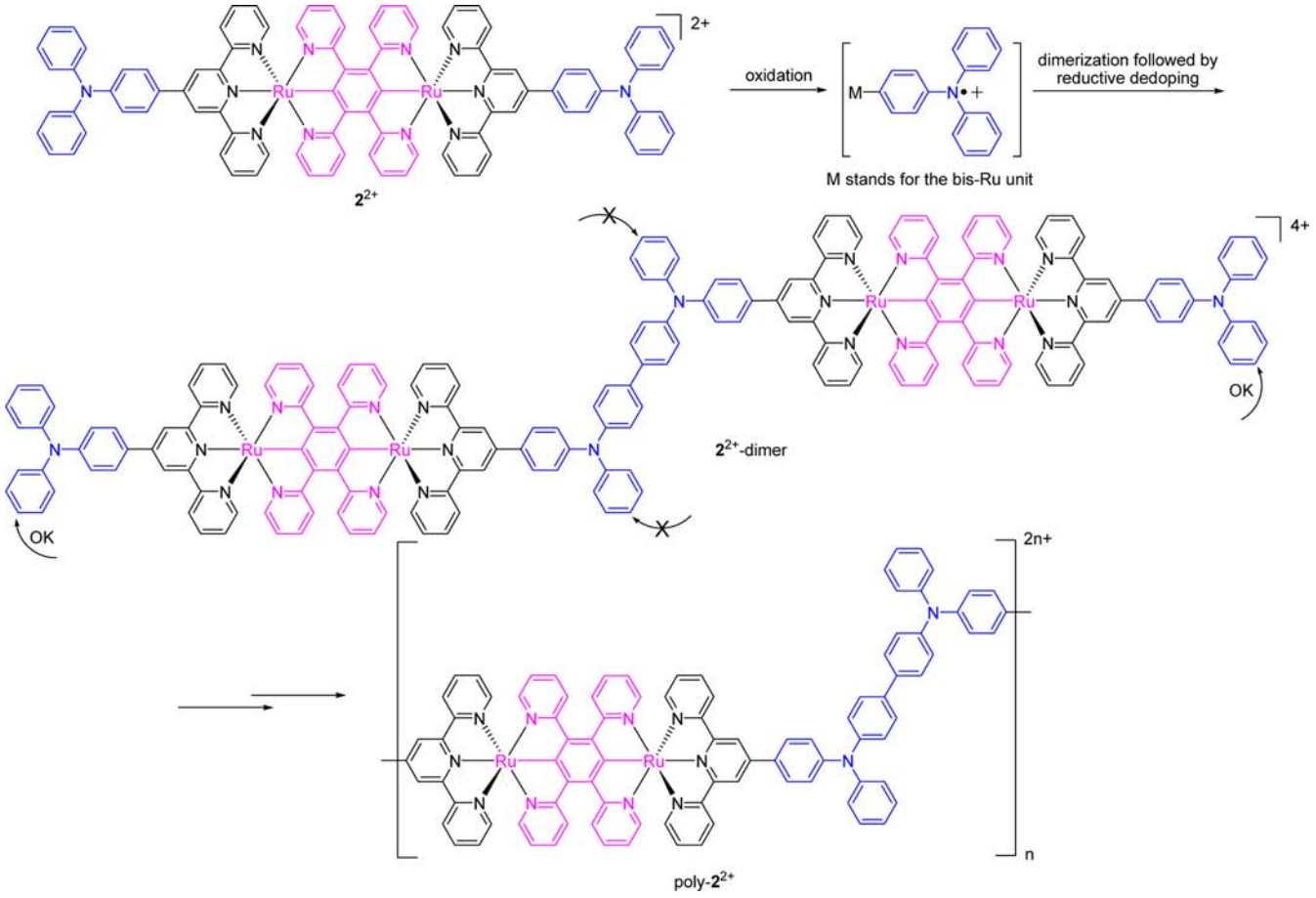

Figure 11. Proposed electropolymerization mechanism and polymer structure.

parallel to and opposite the counter electrode. During the spectroelectrochemistry measurement, a potential was applied on the ITO electrode deposited with the polymeric film by the CHI 620D potentiostat, and the absorption spectra were recorded using a PE Lambda 750 UV/vis/NIR spectrophotometer.

SEM Measurements. Prior to measurement, an ultrathin conductive Au coating was deposited on the top of the polymeric films on ITO glass electrodes by low vacuum sputter coating of the sample. Images were obtained using a field-emission microscope (JEOL S-4800) operated at an acceleration voltage of 10 kV.

XPS Measurements. XPS spectroscopy data were obtained with an ESCALab220i-XL electron spectrometer from VG Scientific using 300 W Al Kα radiation. The base pressure was about 3×10^{-9} mbar. The binding energies were referenced to the C1s line at 284.8 eV from adventitious carbon.

Synthesis. NMR spectra were recorded in the designated solvent on Bruker Avance 400 MHz spectrometer. Spectra are reported in ppm values from residual protons of the deuterated solvent. No distinct NMR spectra have been recorded for complexes **1**$(PF_6)_2$ and **2**$(PF_6)_2$, possibly because of the presence of a small amount of paramagnetic species. Mass data were obtained with a Bruker Daltonics Inc. Apex II FT-ICR or Autoflex III MALDI-TOF mass spectrometer. The matrix for MALDI-TOF measurement is α-cyano-4-hydroxycinnamic acid. Microanalysis was carried out using a Flash EA 1112 or Carlo Erba 1106 analyzer at the Institute of Chemistry, Chinese Academy of Sciences.

4′-(*p*-*N*,*N*-diphenylamino)phenyl-2,2′:6′,2″-terpyridine (Nptpy). To an oven-dried pressure vessel were added 4′-*p*-bromophenyl-2,2′:6′,2″-terpyridine[26] (1.0 mmol, 388 mg), diphenylamine (1.5 mmol, 254 mg), and 30 mL of dry toluene. The solution was bubbled with N_2 for 10 min, followed by the addition of $Pd_2(dba)_3$ (0.020 mmol, 18 mg), dppf (0.020 mmol, 11 mg), and NaO^{t}Bu (1.2 mmol, 115 mg). The mixture was stirred under N_2 at 140 °C for 30 h. After cooling down to room temperature, the solvent was removed under reduced pressure. The product was purified through flash column chromatography on silica gel using a mixture of CH_2Cl_2/ethyl acetate/NH_4OH (30/3/0.1) as the eluent. The desired product 4′-(*p*-*N*,*N*-diphenylamino)phenyl-2,2′:6′,2″-terpyridine[27] (Nptpy) was obtained as a yellow solid (220 mg, 46%). ^{1}H NMR (400 MHz, $CDCl_3$): δ 7.07 (t, J = 7.6 Hz, 2H), 7.16 (t, J = 7.2 Hz, 6H), 7.29 (d, J = 8.0 Hz, 4H), 7.32−7.35 (m, 2H), 7.78 (d, J = 8.8 Hz, 2H), 7.87 (t, J = 8.0 Hz, 2H), 8.65 (d, J = 8.0, Hz, 2H), 8.70 (d, J = 7.6 Hz, 4H). MALDI-MS: 477.3 for $[M + H]^+$.

Synthesis of [(Nptpy)RuCl$_3$]. To 50 mL of dry ethanol were added ligand Nptpy (0.50 mmol, 238 mg) and $RuCl_3 \cdot 3H_2O$ (0.50 mmol, 130 mg). The mixture was refluxed for 4 h before cooling down to room temperature. The product $[Ru(Nptpy)Cl_3]$ was obtained after filtering and washing with water and ether (256 mg, 75%). This product was used for the next transformation without further purification.

Synthesis of [(Nptpy)$_2$Ru$_2$(tppyr)](PF$_6$)$_2$ (1^{2+}). To 20 mL of dry acetone were added the above prepared $[Ru(Nptpy)Cl_3]$ (0.060 mmol, 41 mg) and AgOTf (0.20 mmol, 52 mg). The mixture was refluxed for 3 h before cooling to room temperature. The resulting AgCl precipitate was removed by filtration. The filtrate was concentrated to dryness. To the residue were added 1,3,6,8-tetra(pyridin-2-yl)pyrene[19] (tppyrH_2, 0.030 mmol, 15.4 mg), 10 mL of DMF, and 10 mL of ^{t}BuOH (10 mL). The mixture was refluxed under microwave heating (power = 375 W) for 30 min. After cooling to room temperature, the solvent was removed under reduced pressure. The residue was dissolved in 2 mL of methanol, followed by the addition of an excess of KPF_6. The resulting precipitate was collected by filtering and washing with water and Et_2O. The obtained solid was subjected to flash column chromatography on silica gel

dx.doi.org/10.1021/ic401288g | *Inorg. Chem.* 2013, 52, 10000−10008

(eluent: CH_3CN/H_2O/aq. KNO_3, 150/20/0.1) followed by anion exchange with KPF_6. The desired product $[\mathbf{1}](PF_6)_2$ was obtained after filtration and washing with water and Et_2O as a black solid (26 mg, 44%). MALDI-MS (Supporting Information, Figure S6): 1808.2 for $[M - PF_6 - H]^+$, 1663.4 for $[M - 2PF_6 - H]^{2+}$. Anal. Calcd for $C_{102}H_{68}F_{12}N_{12}P_2Ru_2{\cdot}Et_2O{\cdot}2H_2O$: C, 61.68; H, 4.00; N, 8.14. Found: C, 61.53; H, 4.31; N, 7.97.

Synthesis of $[(Nptpy)_2Ru_2(tpb)](PF_6)_2$ (2^{2+}). To 20 mL of dry acetone were added $[Ru(Nptpy)Cl_3]$ (0.060 mmol, 41 mg) and AgOTf (0.20 mmol, 52 mg). The mixture was refluxed for 3 h before cooling to room temperature. After standing for 1 h, the resulting white AgCl precipitate was removed by filtration. The filtrate was concentrated to dryness. To the residue were added 1,2,4,5-tetra(pyridin-2-yl)benzene[20] ($tpbH_2$, 0.030 mmol, 11 mg), DMF (8 mL), and *t*-BuOH (8 mL). The mixture was bubbled with nitrogen for 30 min before the vial was capped and heated at 140 °C for 48 h. After cooling to room temperature, the solvent was removed under reduced pressure. The residue was dissolved in 2 mL of methanol, followed by the addition of an excess of aq. KPF_6. The resulting precipitate was collected by filtering and washing with water and Et_2O. The crude solid was purified by silica gel chromatography (eluent: CH_3CN/H_2O/aq.KNO_3 100/20/0.1), followed by anion exchange with KPF_6, to give 24 mg of $[\mathbf{2}](PF_6)_2$ as a black solid in 43% yield. MALDI-MS (Supporting Information, Figure S7): 1685.4 for $[M - PF_6]^+$, 1539.5 for $[M - 2PF_6]^+$. Anal. Calcd for: $C_{92}H_{64}F_{12}N_{12}P_2Ru_2.4H_2O$: C, 58.11; H, 3.82; N, 8.84; Found: C, 58.00; H, 3.50; N, 8.82.

■ ASSOCIATED CONTENT

Ⓢ Supporting Information

Spectral changes during oxidative titration of $\mathbf{1}^{2+}$ and $\mathbf{2}^{2+}$ in acetonitrile, transmittance changes during electrochromic switching of poly-$\mathbf{1}^{2+}$/ITO and poly-$\mathbf{2}^{2+}$/ITO film with low surface coverage, and MALDI-MS spectra. This material is available free of charge via the Internet at http://pubs.acs.org.

■ AUTHOR INFORMATION

Corresponding Author

*E-mail: zhongyuwu@iccas.ac.cn.

Notes

The authors declare no competing financial interest.

■ ACKNOWLEDGMENTS

We thank the National Natural Science Foundation of China (Grants 91227104, 21002104, 21271176, and 212210017), the National Basic Research 973 program of China (Grant 2011CB932301), and Institute of Chemistry, Chinese Academy of Sciences ("100 Talent" Program and Grant CMS-PY-201230) for funding support.

■ REFERENCES

(1) (a) Mortimer, R. J. *Chem. Soc. Rev.* **1997**, *26*, 147. (b) Sonmez, G. *Chem. Commun.* **2005**, 5251. (c) Beaujuge, P. M.; Reynolds, J. R. *Chem. Rev.* **2010**, *110*, 268. (d) Gunbas, G.; Toppare, L. *Chem. Commun.* **2012**, *48*, 1083. (e) Thakur, V. K.; Ding, G.; Ma, J.; Lee, P. S.; Lu, X. *Adv. Mater.* **2012**, *24*, 4071.

(2) (a) Rosseinsky, D. R.; Mortimer, R. J. *Adv. Mater.* **2001**, *13*, 783. (b) Akita, M.; Koike, T. *Dalton Trans.* **2008**, 3523. (c) Sonmez, G.; Sonmez, H. *J. Mater. Chem.* **2006**, *16*, 2473. (d) Tuccitto, N.; Ferri, V.; Cavazzini, M.; Quici, S.; Zhavnerko, G.; Licciardello, A.; Rampi, M. A. *Nat. Mater.* **2009**, *8*, 41. (e) Ying, J.-W.; Liu, I. P.-C.; Xi, B.; Song, Y.; Campana, C.; Zuo, J.-L.; Ren, T. *Angew. Chem., Int. Ed.* **2010**, *49*, 954.

(3) (a) Maier, A.; Rabindranath, A. R.; Tieke, B. *Adv. Mater.* **2009**, *21*, 959. (b) Maier, A.; Cheng, K.; Savych, J.; Tieke, B. *ACS Appl. Mater. Interfaces* **2011**, *3*, 2710. (c) Tieke, B. *Curr. Opin. Colloid Interface Sci.* **2011**, *16*, 499.

(4) (a) Groenendaal, L. B.; Zotti, G.; Aubert, P.-H.; Waybright, S. M.; Reynolds, J. R. *Adv. Mater.* **2003**, *15*, 855. (b) Heinze, J.; Frontana-Uribe, B. A.; Ludwigs, S. *Chem. Rev.* **2010**, *110*, 4724. (c) Friebe, C.; Hager, M. D.; Winter, A.; Schubert, U. S. *Adv. Mater.* **2012**, *24*, 332.

(5) (a) Bach, U.; Corr, D.; Lupo, D.; Pichot, F.; Ryan, M. *Adv. Mater.* **2002**, *11*, 845. (b) Lee, S.-H.; Deshpande, R.; Parilla, P. A.; Jones, K. M.; To, B.; Mahan, A. H.; Dillon, A. C. *Adv. Mater.* **2006**, *18*, 763.

(6) (a) Li, M.; Patra, A.; Sheynin, Y.; Bendikov, M. *Adv. Mater.* **2009**, *21*, 1707. (b) Amb, C. M.; Dyer, A. L.; Reynolds, J. R. *Chem. Mater.* **2011**, *23*, 397. (c) Liu, W.; Huang, W.; Pink, M.; Lee, D. *J. Am. Chem. Soc.* **2010**, *132*, 11844.

(7) (a) Leasure, R. M.; Ou, W.; Moss, J. A.; Linton, R. W.; Meyer, T. J. *Chem. Mater.* **1996**, *8*, 264. (b) Bernhard, S.; Goldsmith, J. I.; Takada, K.; Abruña, H. D. *Inorg. Chem.* **2003**, *42*, 4389. (c) Biancardo, M.; Schwab, P. F. H.; Argazzi, R.; Bignozzi, C. A. *Inorg. Chem.* **2003**, *42*, 3966. (d) Han, F. S.; Higuchi, M.; Kurth, D. G. *Adv. Mater.* **2007**, *19*, 3928. (e) Han, F. S.; Higuchi, M.; Kurth, D. G. *J. Am. Chem. Soc.* **2008**, *130*, 2073. (f) Motiei, L.; Lahav, M.; Freeman, D.; van der Boom, M. E. *J. Am. Chem. Soc.* **2009**, *131*, 3468. (g) Powell, A. P.; Bielawski, C. W.; Cowley, A. H. *J. Am. Chem. Soc.* **2009**, *131*, 18232. (h) Milum, K. M.; Kim, Y. N.; Holliday, B. J. *Chem. Mater.* **2010**, *22*, 2414. (i) Powell, A. P.; Bielawski, C. W.; Cowley, A. H. *J. Am. Chem. Soc.* **2010**, *132*, 10184. (j) Puodziukynaite, E.; Oberst, J. L.; Dyer, A. L.; Reynolds, J. R. *J. Am. Chem. Soc.* **2012**, *134*, 968. (k) Hossain, M. D.; Sato, T.; Higuchi, M. H. *Chem.—Asian. J.* **2013**, *8*, 76.

(8) (a) Chandrasekhar, P.; Zay, B. J.; Birur, G. C.; Rawal, S.; Pierson, E. A.; Kauder, L.; Swanson, T. *Adv. Funct. Mater.* **2002**, *12*, 95. (b) Garcíña-Canadas, J.; Meacham, A. P.; Peter, L. M.; Ward, M. D. *Angew. Chem., Int. Ed.* **2003**, *42*, 3011. (c) Ward, M. D. *J. Solid State Electrochem.* **2005**, *9*, 778. (d) Lin, W.; Zheng, Y.; Zhang, J.; Wan, X. *Macromolecules* **2011**, *44*, 5146. (e) Qian, G.; Abu, H.; Wang, Z. Y. *J. Mater. Chem.* **2011**, *21*, 7678.

(9) (a) Fablan, J.; Nakazumi, H.; Matsuoka, M. *Chem. Rev.* **1992**, *92*, 1197. (b) Qian, G.; Wang, Z. Y. *Chem.—Asian J.* **2010**, *5*, 1006. (c) Kaim, W. *Coord. Chem. Rev.* **2011**, *255*, 2503.

(10) (a) Chang, C.-W.; Liou, G.-S. *J. Mater. Chem.* **2008**, *18*, 5638. (b) Yen, H.-J.; Liou, G.-S. *J. Mater. Chem.* **2010**, *20*, 9886. (c) Yen, H.-J.; Lin, K.-Y.; Liou, G.-S. *J. Mater. Chem.* **2011**, *21*, 6230. (d) Yen, H.-J.; Lin, K.-Y.; Liou, G.-S. *Chem. Mater.* **2011**, *23*, 1874.

(11) Robin, M. B.; Day, P. *Adv. Inorg. Chem. Radiochem.* **1967**, *8*, 357.

(12) (a) Abruña, H. D.; Denisevich, P.; Umaña, M.; Meyer, T. J.; Murray, R. W. *J. Am. Chem. Soc.* **1981**, *103*, 1. (b) Denisevich, P.; Abruña, H. D.; Leidner, C. R.; Meyer, T. J.; Murray, R. W. *Inorg. Chem.* **1982**, *21*, 2153. (c) Potts, K. T.; Usifer, D. A.; Guadalupe, A. R.; Abruña, H. D. *J. Am. Chem. Soc.* **1987**, *109*, 3961. (d) Guadalupe, A. R.; Usifer, D. A.; Potts, K. T.; Hurrell, H. C.; Mogstad, A.-E.; Abruña, H. D. *J. Am. Chem. Soc.* **1988**, *110*, 3462. (e) Nie, H.-J.; Yao, J.; Zhong, Y.-W. *J. Org. Chem.* **2011**, *76*, 4771. (f) Zhong, Y.-W.; Yao, C.-J.; Nie, H.-J. *Coord. Chem. Rev.* **2013**, *257*, 1357.

(13) (a) Yao, C.-J.; Zhong, Y.-W.; Nie, H.-J.; Abruña, H. D.; Yao, J. *J. Am. Chem. Soc.* **2011**, *133*, 20720. (b) Yao, C.-J.; Yao, J.; Zhong, Y.-W. *Inorg. Chem.* **2012**, *51*, 6259.

(14) (a) Djukic, J.-P.; Sortais, J.-B.; Barloy, L.; Pfeffer, M. *Eur. J. Inorg. Chem.* **2009**, 817. (b) Wadman, S. H.; Havenith, R. W. A.; Hartl, F.; Lutz, M.; Spek, A. L.; van Klink, G. P. M.; van Koten, G. *Inorg. Chem.* **2009**, *48*, 5685. (c) Bomben, P. G.; Koivisto, B. D.; Berlinguette, C. P. *Inorg. Chem.* **2010**, *49*, 4960. (d) Zhang, Y.-M.; Shao, J.-Y.; Yao, C.-J.; Zhong, Y.-W. *Dalton Trans.* **2012**, *41*, 9280. (e) Yao, C.-J.; Zheng, R.-H.; Shi, Q.; Zhong, Y.-W.; Yao, J. *Chem. Commun.* **2012**, *48*, 5680.

(15) (a) D'Alessandro, D. M.; Keene, F. R. *Chem. Rev.* **2006**, *106*, 2270. (b) Kaim, W.; Lahiri, G. K. *Angew. Chem., Int. Ed.* **2007**, *46*, 1778. (c) Lincke, K.; Frellsen, A. F.; Parkar, C. R.; Bond, A. D.; Hammerich, O.; Nielsen, M. B. *Angew. Chem., Int. Ed.* **2012**, *51*, 6099.

(16) (a) LeClair, G.; Wang, Z. Y. *J. Solid. State Electrochem.* **2009**, *13*, 365. (b) Qi, Y. H.; Desjardins, P.; Meng, X. S.; Wang, Z. Y. *Opt. Mater.* **2002**, *21*, 255. (c) Argun, A. A.; Aubert, P.-H.; Thompson, B. C.; Schwendeman, I.; Gaupp, C. L.; Hwang, J.; Pinto, N.; Tanner, D. B.; MacDiarmid, A. G.; Reynolds, J. R. *Chem. Mater.* **2004**, *16*, 4401. (d) Kondo, Y.; Tanabe, H.; Kudo, H.; Nakano, K.; Otake, T. *Materials*

2011, *4*, 2171. (e) Witker, D.; Reynolds, J. R. *Macromolecules* **2005**, *38*, 7636.
(17) (a) Wu, S.-H.; Burkhardt, S. E.; Zhong, Y.-W.; Abruna, H. D. *Inorg. Chem.* **2012**, *51*, 13312. (b) Flores-Torres, S.; Hutchison, G. R.; Stoltzberg, L. J.; Abruna, H. D. *J. Am. Chem. Soc.* **2006**, *128*, 1513.
(18) (a) Seo, E. T.; Nelson, R. F.; Fritsch, J. M.; Marcoux, L. S.; Leedy, D. W.; Adams, R. N. *J. Am. Chem. Soc.* **1966**, *88*, 3498. (b) Creason, S. C.; Wheeler, J.; Nelson, R. F. *J. Org. Chem.* **1972**, *37*, 4440. (c) Petr, A.; Kvarnstrom, C.; Dunsch, L.; Ivaska, A. *Synth. Met.* **2000**, *108*, 245.
(19) Yao, C.-J.; Sui, L.-Z.; Xie, H.-Y.; Xiao, W.-J.; Zhong, Y.-W.; Yao, J. *Inorg. Chem.* **2010**, *49*, 8347.
(20) (a) Yao, C.-J.; Zhong, Y.-W.; Yao, J. *J. Am. Chem. Soc.* **2011**, *133*, 15697. (b) Sui, L.-Z.; Yang, W.-W.; Yao, C.-J.; Xie, H.-Y.; Zhong, Y.-W. *Inorg. Chem.* **2012**, *51*, 1590.
(21) Lambert, C.; Noll, G. *J. Am. Chem. Soc.* **1999**, *121*, 8434.
(22) The coloration efficiency was determined according to equations $CE(\lambda) = \Delta OD/Q_d$ and $\Delta OD = \log[T_b/T_c]$, where OD is optical density, Q_d is the injected/ejected charge density (C/cm^2), and T_b and T_c are the transmittance in the bleached and colored states at indicated wavelength.
(23) (a) Leung, M.-k.; Chou, M.-Y.; Su, Y. O.; Chiang, C. L.; Chen, H.-L.; Yang, C. F.; Yang, C.-C.; Lin, C.-C.; Chen, H. T. *Org. Lett.* **2003**, *5*, 839. (b) Otero, L.; Sereno, L.; Fungo, F.; Liao, Y.-L.; Lin, C.-Y.; Wong, K.-T. *Chem. Mater.* **2006**, *18*, 3495. (c) Natera, J.; Otero, L.; Sereno, L.; Fungo, F.; Wang, N.-S.; Tsai, Y.-M.; Hwu, T.-Y.; Wong, K.-T. *Macromolecules* **2007**, *40*, 4456. (d) Chang, C.-C.; Leung, M.-k. *Chem. Mater.* **2006**, *20*, 5816.
(24) All electrochromic properties in this paper were studied under ambient conditions. Film stabilities will be improved if measured under a N_2 atmosphere. Besides, response time and contrast ratio will be possibly improved by changing the electrodes and electrolyte used.
(25) (a) Creutz, C.; Taube, H. *J. Am. Chem. Soc.* **1969**, *91*, 3988. (b) Gagliardo, M.; Amijs, C. H. M.; Lutz, M.; Spek, A. L.; Havenith, R. W. A.; Hartl, F.; van Klink, G. P. M.; van Koten, G. *Inorg. Chem.* **2007**, *46*, 11133. (c) Aguirre-Etcheverry, P.; O'Hare, D. *Chem. Rev.* **2010**, *110*, 4839. (d) Chisholm, M. H.; Lear, B. J. *Chem. Soc. Rev.* **2011**, *40*, 5254. (e) Shao, J.-Y.; Yang, W.-W.; Yao, J.; Zhong, Y.-W. *Inorg. Chem.* **2012**, *51*, 4343.
(26) Wang, J.; Hanan, G. S. *Synlett* **2005**, 1251.
(27) Goodall, W.; Williams, J. A. G. *Chem. Commun.* **2001**, 2514.